Electronic Supplementary Material (ESI) for Journal of Materials Chemistry A.

Unraveling the Role of Single Atom Catalysts on the Charging Behavior of Nonaqueous Mg-CO_2 Batteries: A Combined Density Functional Theory and Machine Learning Approach

Raffiuzzaman Pritom[a], Rahul Jayan[a] and Md Mahbubul Islam*

Department of Mechanical Engineering, Wayne State University, Detroit, MI – 48202, USA

[a] both authors contributed equally towards this work

*Corresponding Author: gy5553@wayne.edu

Table S1. The computed lattice constants of 3d SACs doped N_4, N_3S and N_2S_2 substrates

SACs	TM-N_4	TM-N_3S	TM-N_2S_2
	Å	Å	Å
Sc	8.478	8.596	8.478
Ti	8.420	8.550	8.703
V	8.408	8.530	8.659
Cr	8.370	8.517	8.635
Mn	8.371	8.494	8.620
Fe	8.348	8.468	8.590
Co	8.329	8.449	8.577
Ni	8.327	8.417	8.622
Cu	8.380	8.459	8.486

Table S2. The computed lattice constants of 4d SACs doped N_4, N_3S and N_2S_2 substrates

SACs	TM-N_4	TM-N_3S	TM-N_2S_2
	Å	Å	Å
Y	8.464	8.504	8.527
Zr	8.500	8.497	8.555
Nb	8.465	8.605	8.559
Mo	8.437	8.561	8.702
Tc	8.422	8.528	8.678
Ru	8.390	8.512	8.646
Rh	8.382	8.510	8.646
Pd	8.388	8.518	8.491
Ag	8.432	8.500	8.581

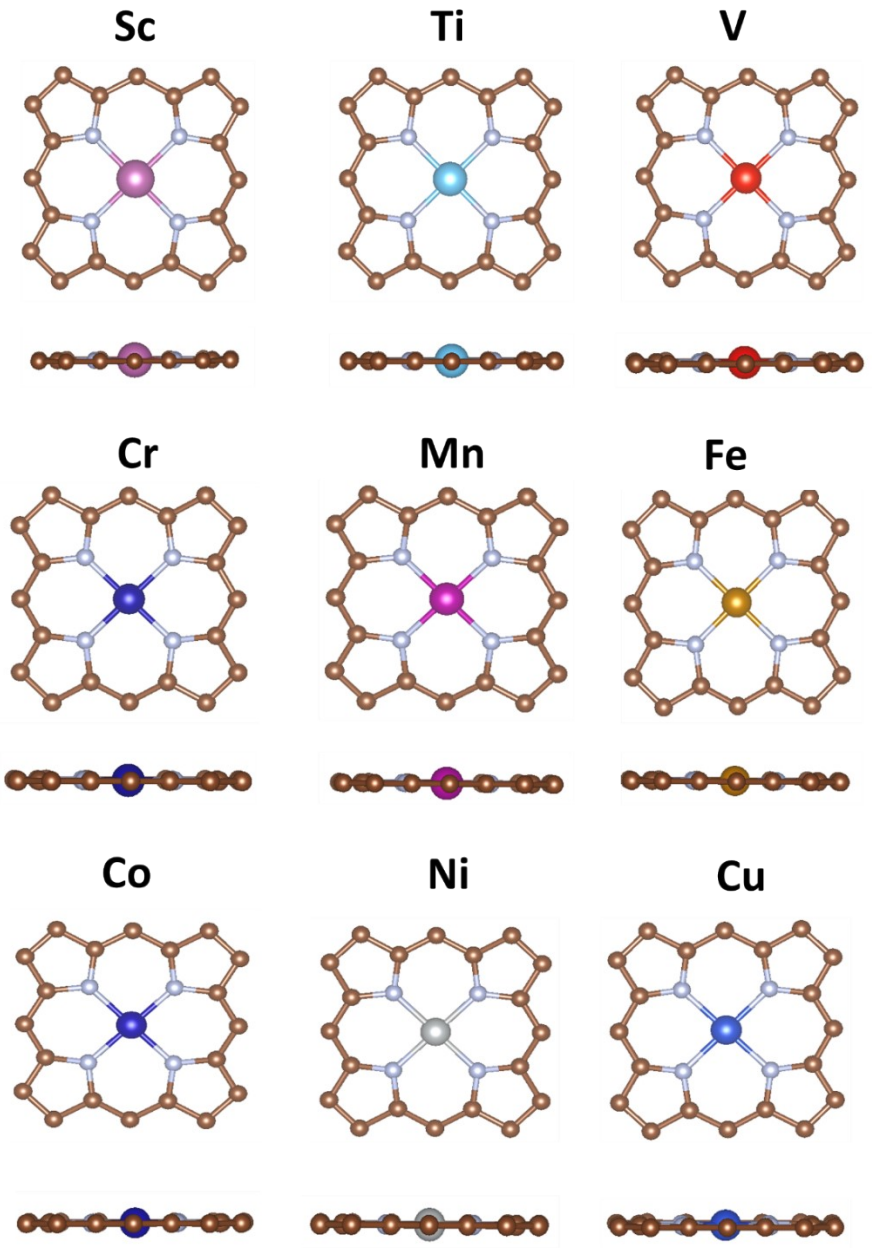

Figure S1. The top and side views of the optimized geometric configurations of 3d SACs doped N_4 environment

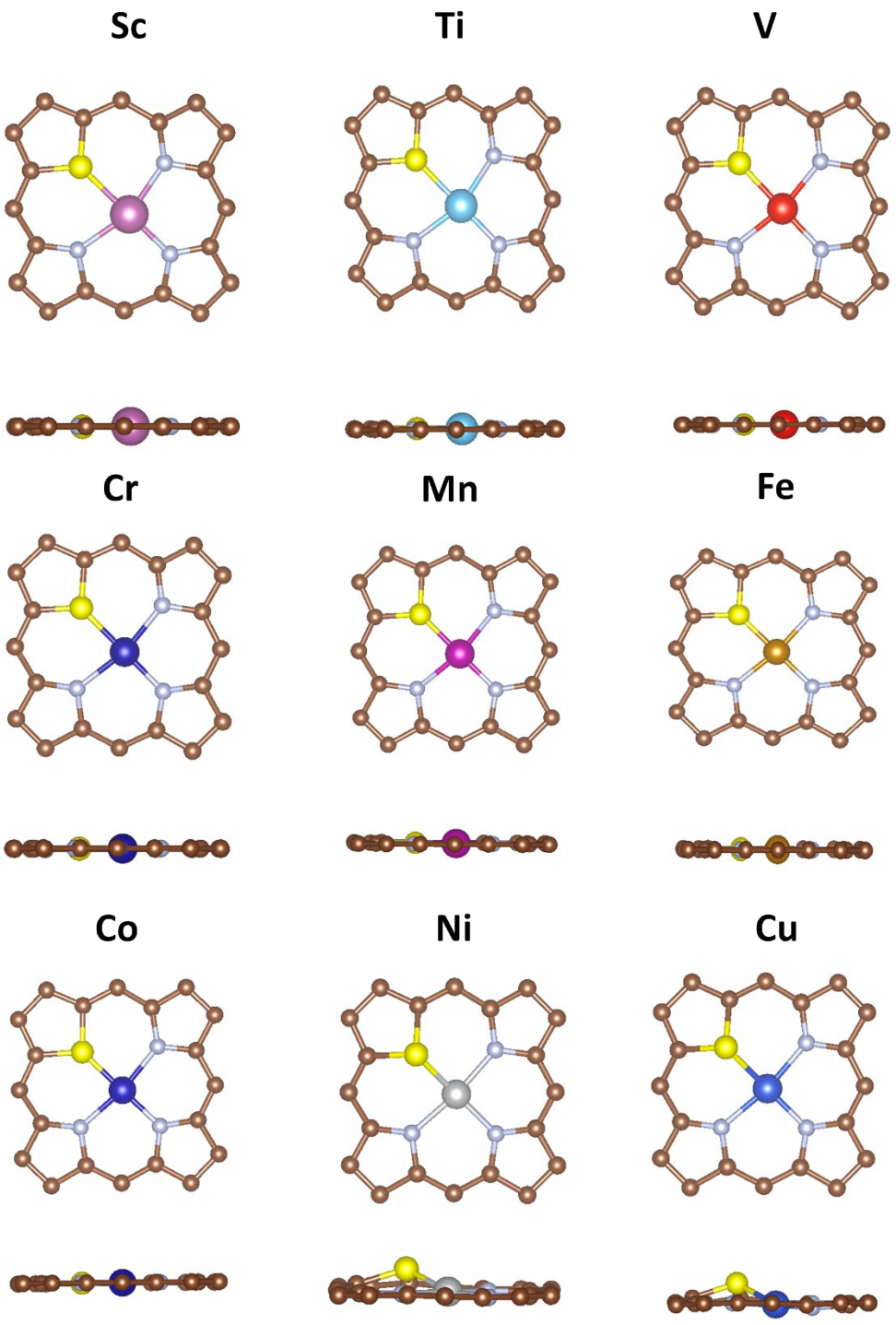

Figure S2. The top and side views of the optimized geometric configurations of 3d SACs doped N_3S environment

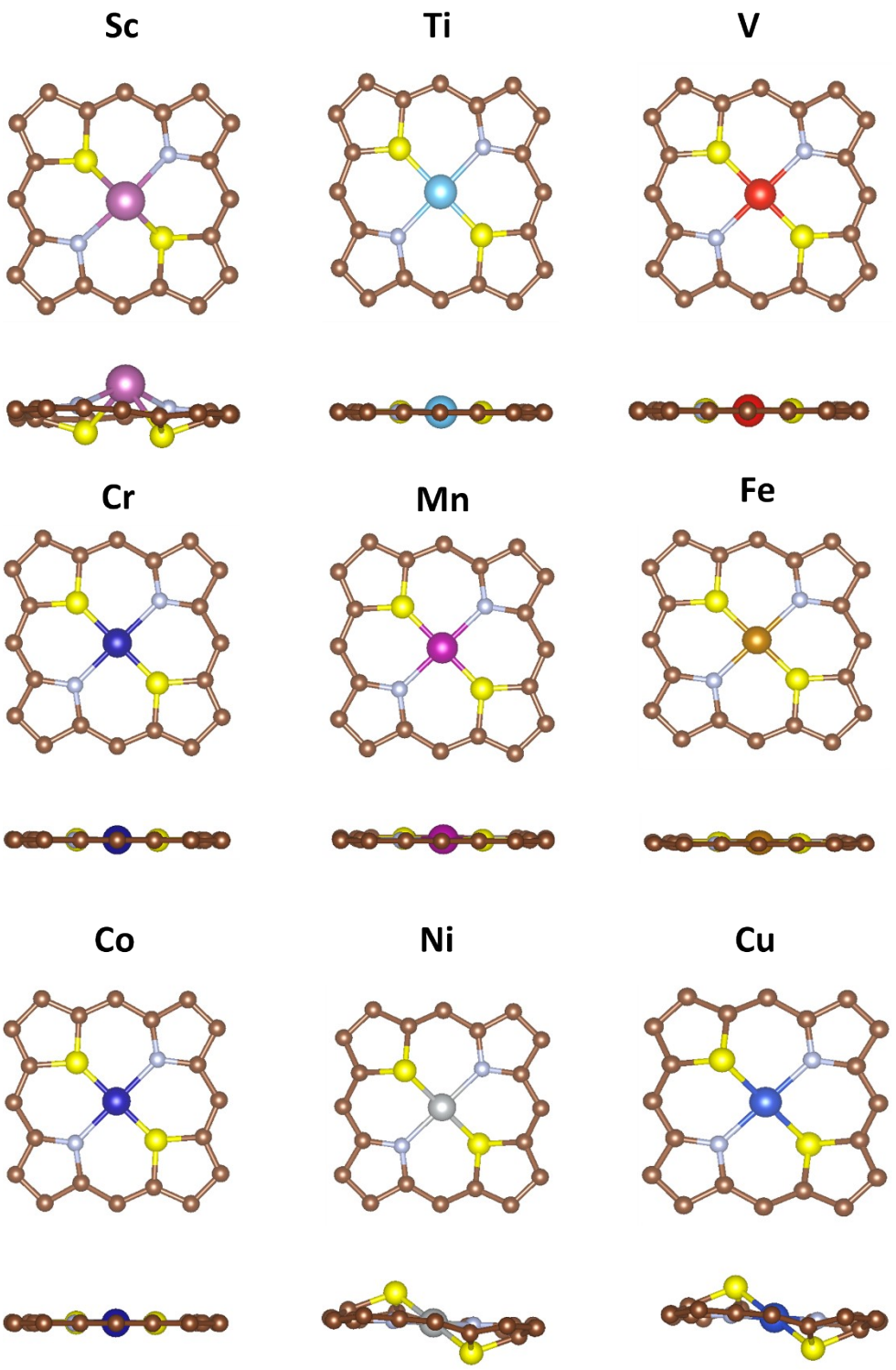

Figure S3. The top and side views of the optimized geometric configurations of 3d SACs doped N_2S_2 environment

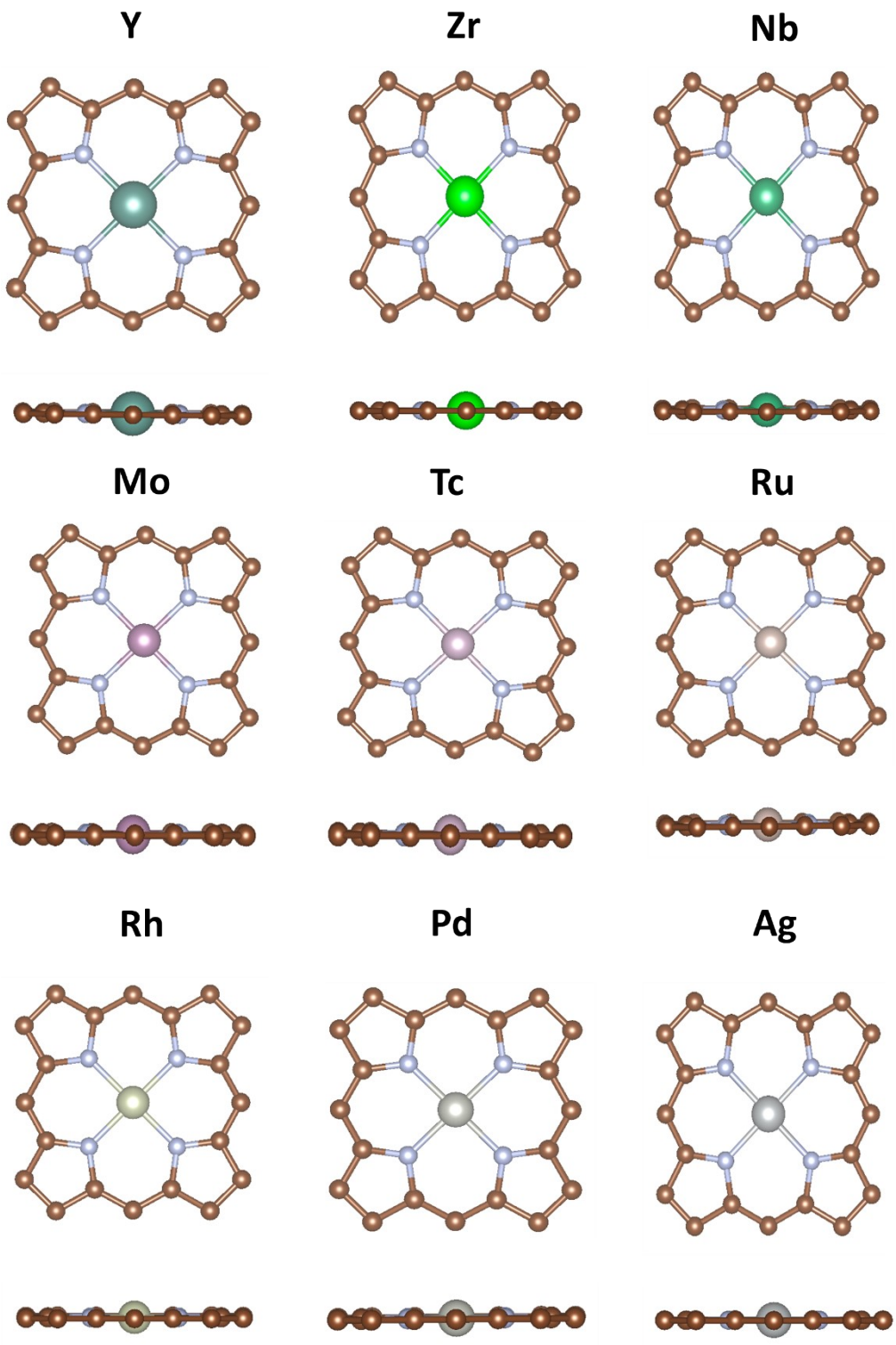

Figure S4. The top and side views of the optimized geometric configurations of 4d SACs doped N_4 environment

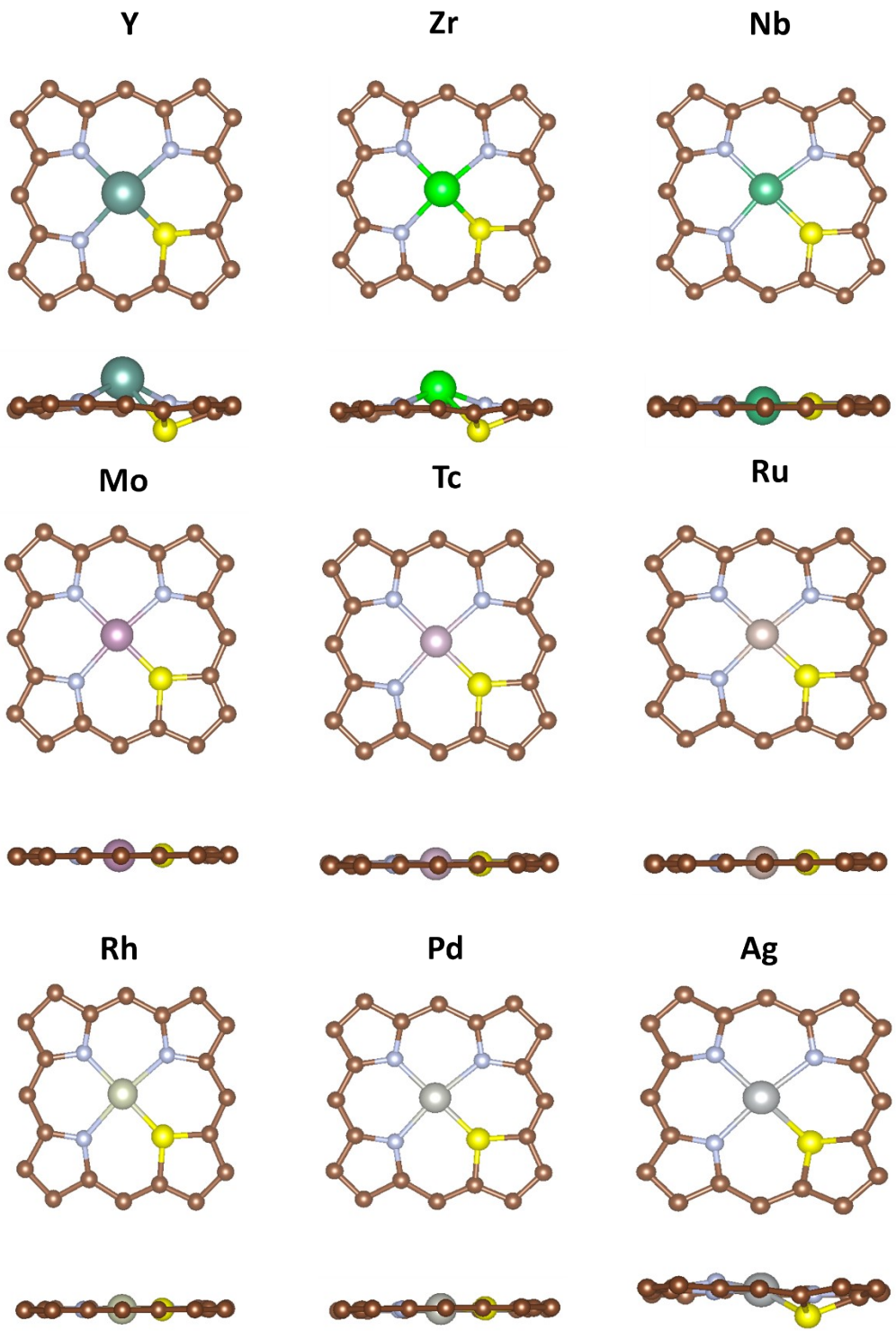

Figure S5. The top and side views of the optimized geometric configurations of 4d SACs doped N_3S environment

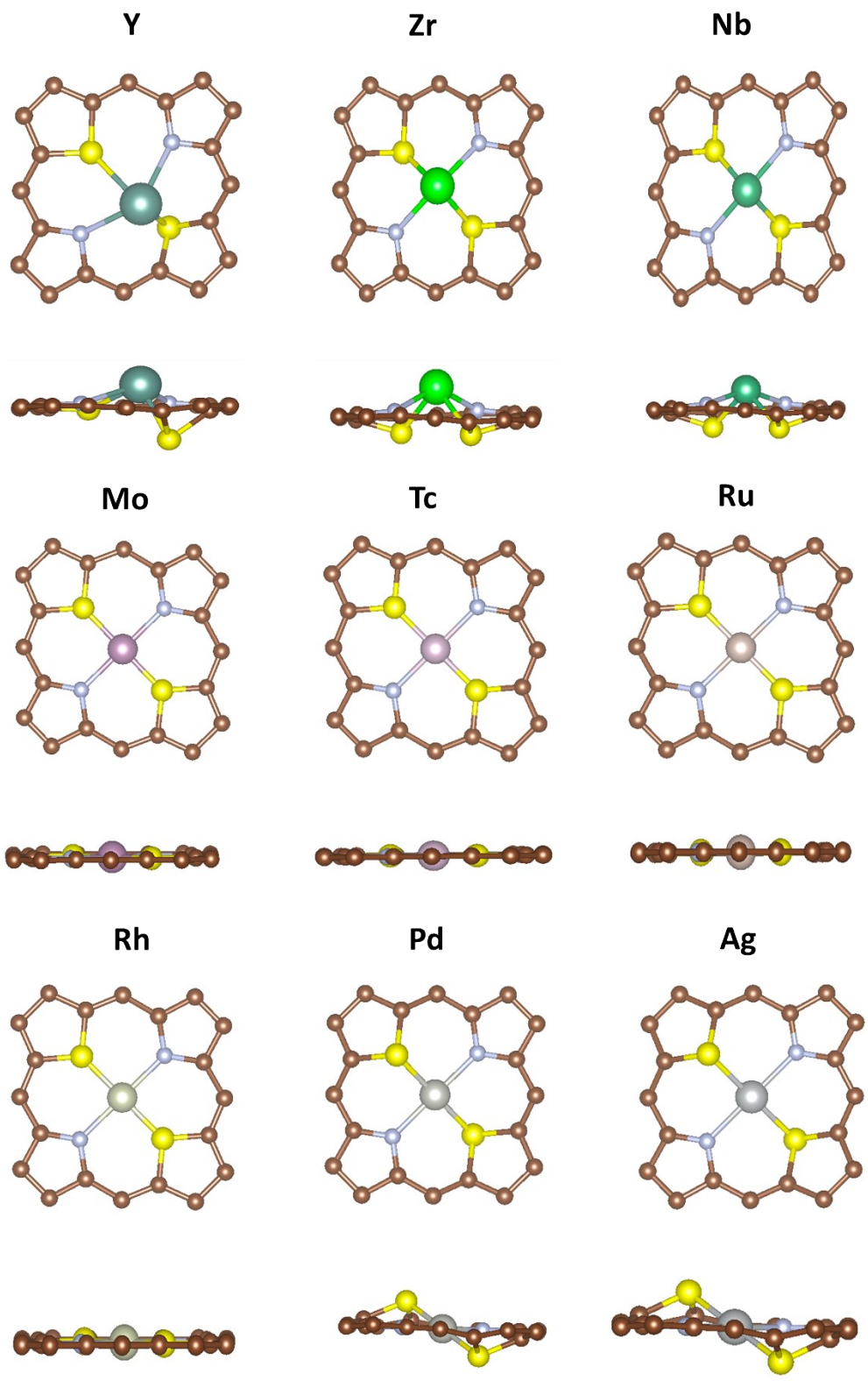

Figure S6. The top and side views of the optimized geometric configurations of 4d SACs doped N_2S_2 environment

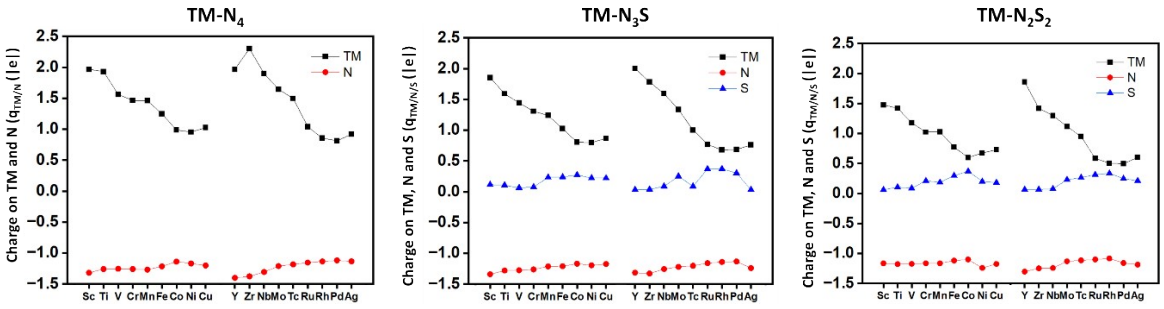

Figure S7. The computed charge transfer of TM, N and S on 3d and 4d SACs doped N_4, N_3S and N_2S_2 substrates

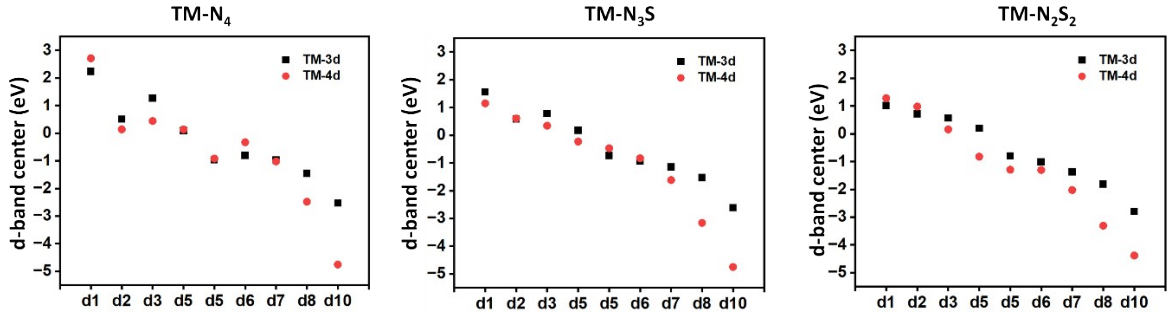

Figure S8. The calculated d-band center of both 3d and 4d SACs doped N_4, N_3S and N_2S_2 substrates

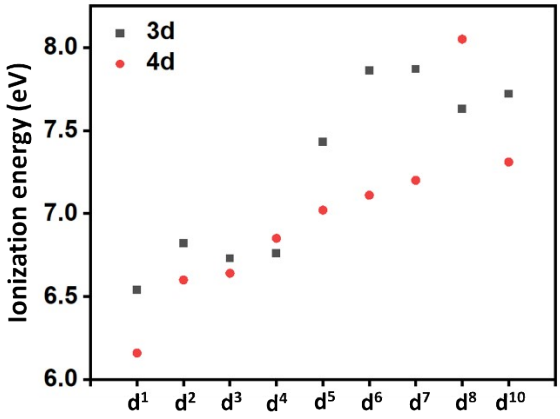

Figure S9. The correlation of ionization energy of both 3d and 4d SACs with the number of d-electrons

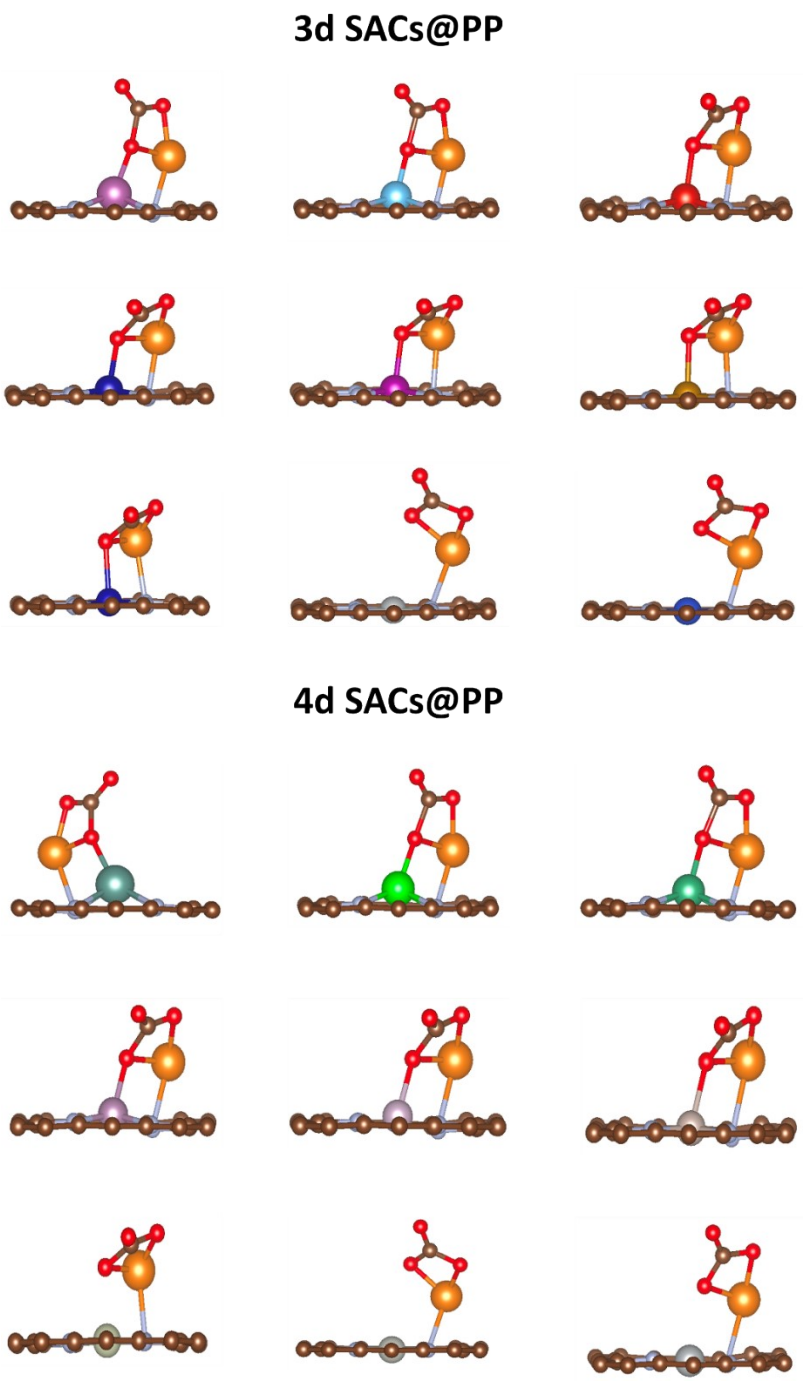

Figure S10. The side views of the optimized geometric configurations of $MgCO_3$ adsorbed on 3d and 4d SACs doped N_4 environment

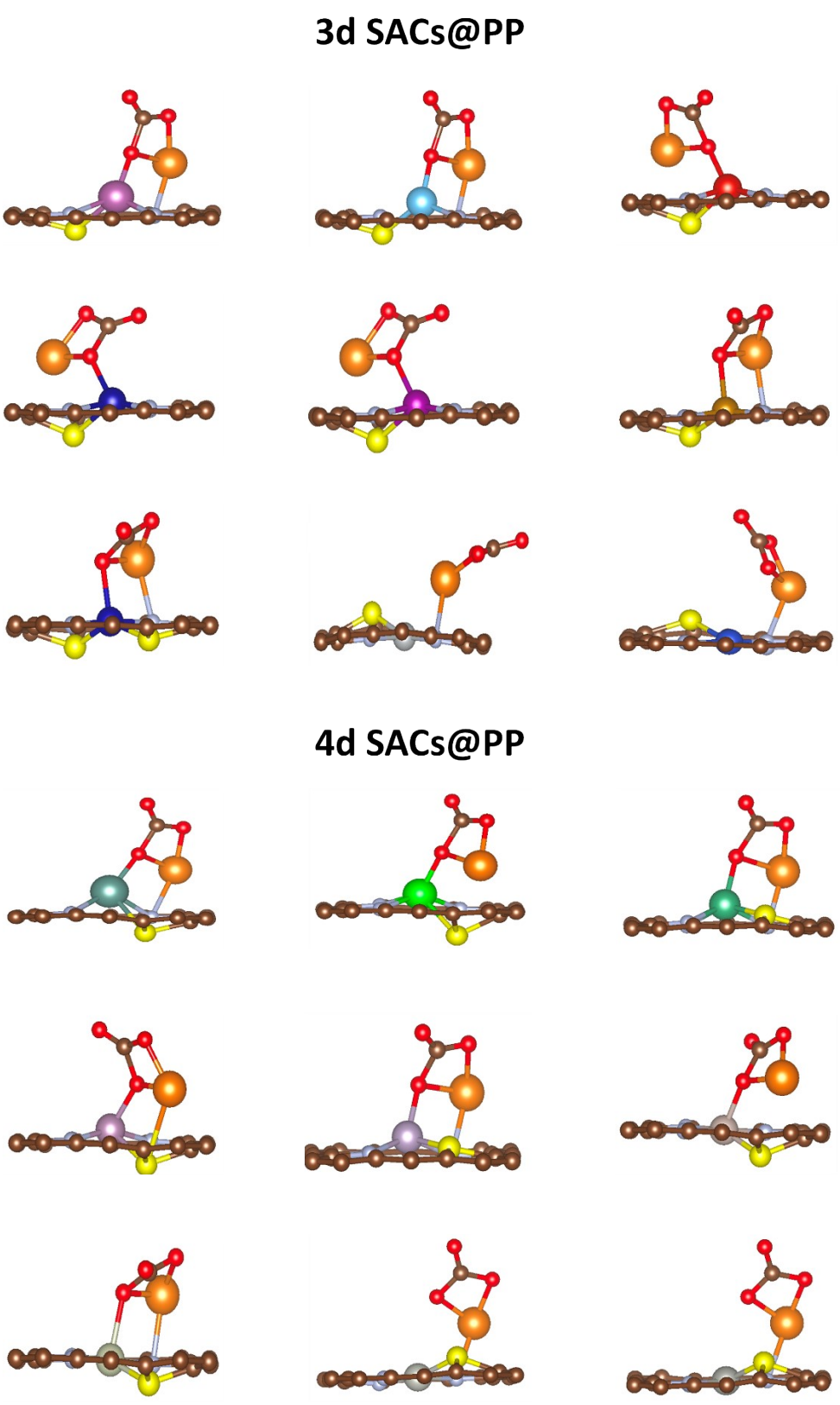

Figure S11. The side views of the optimized geometric configurations of $MgCO_3$ adsorbed on 3d and 4d SACs doped N_3S environment

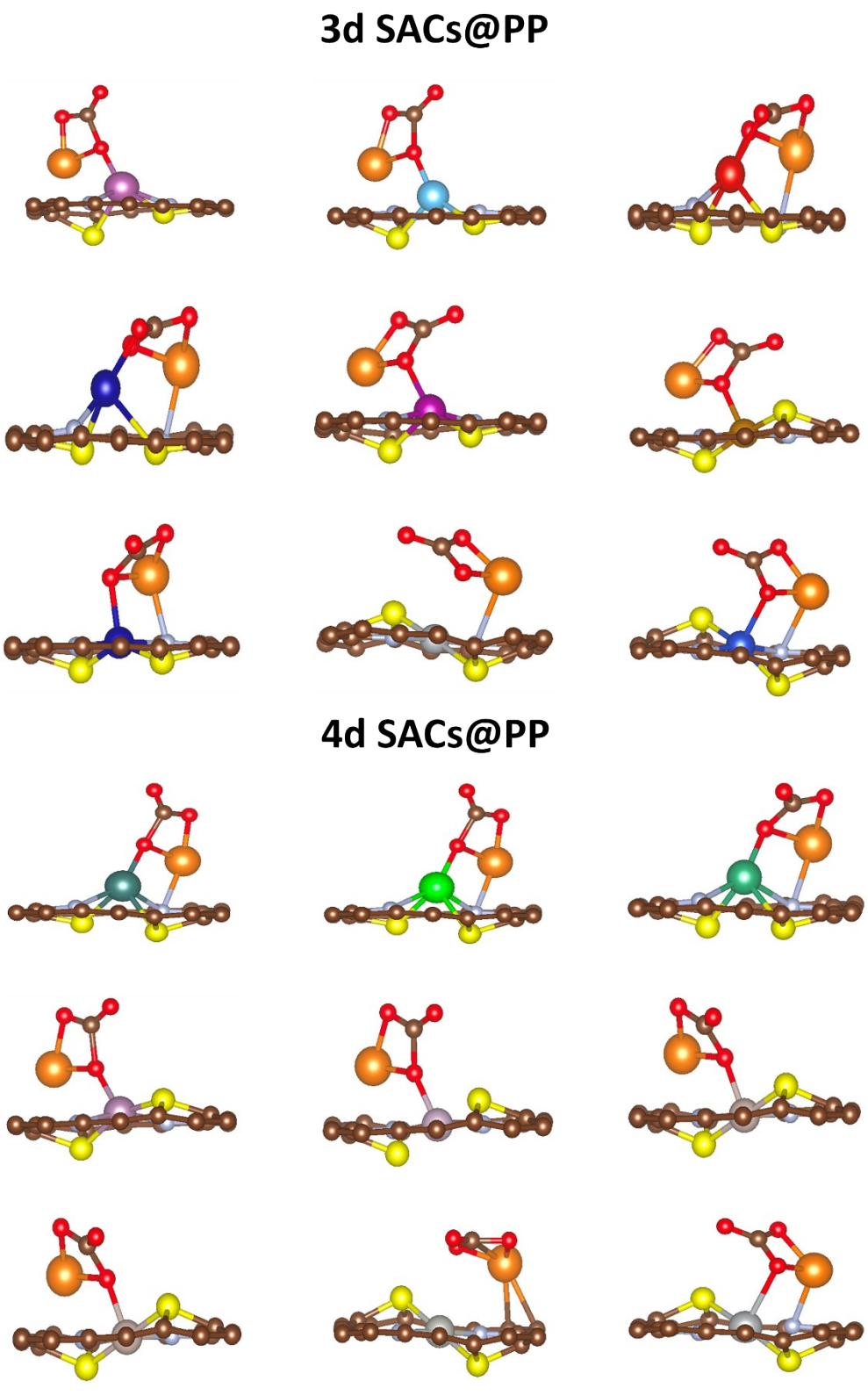

Figure S12. The side views of the optimized geometric configurations of $MgCO_3$ adsorbed on 3d and 4d SACs doped N_2S_2 environment

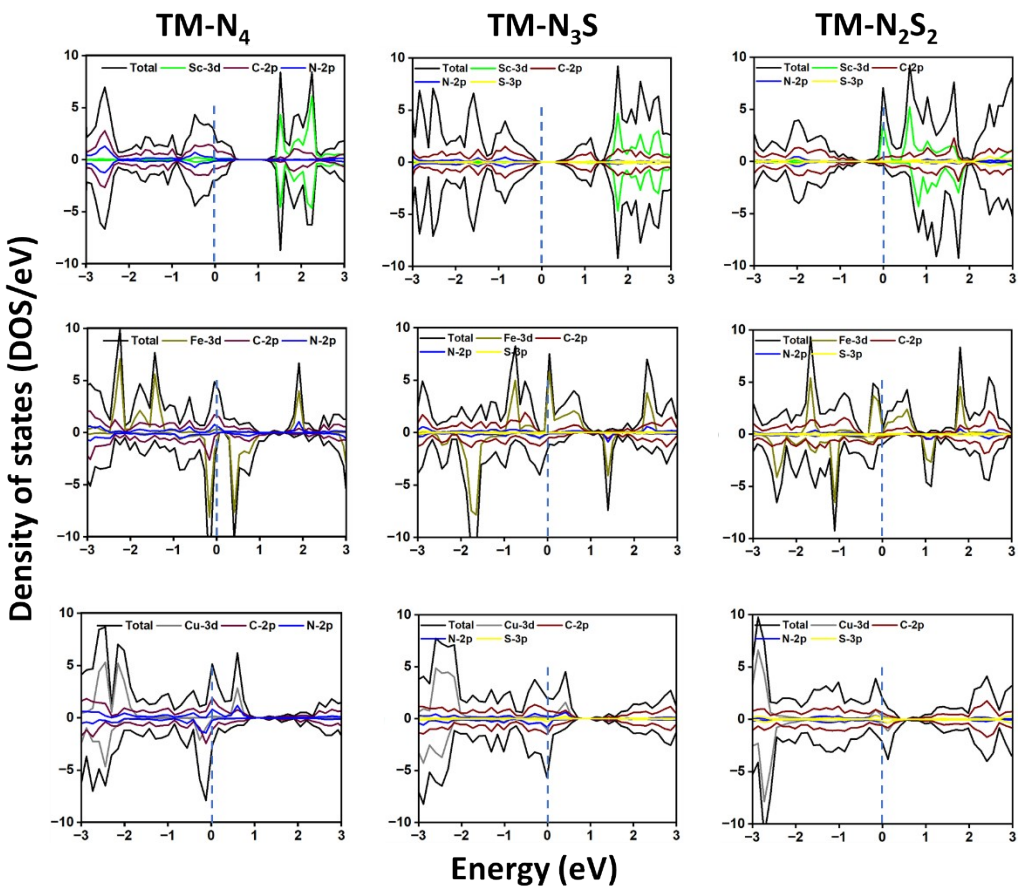

Figure S13. Projected density of states (PDOS) of representative early (Sc), mid (Fe) and late (Cu) 3d-TM doped N_4, N_3S and N_2S_2 substrates

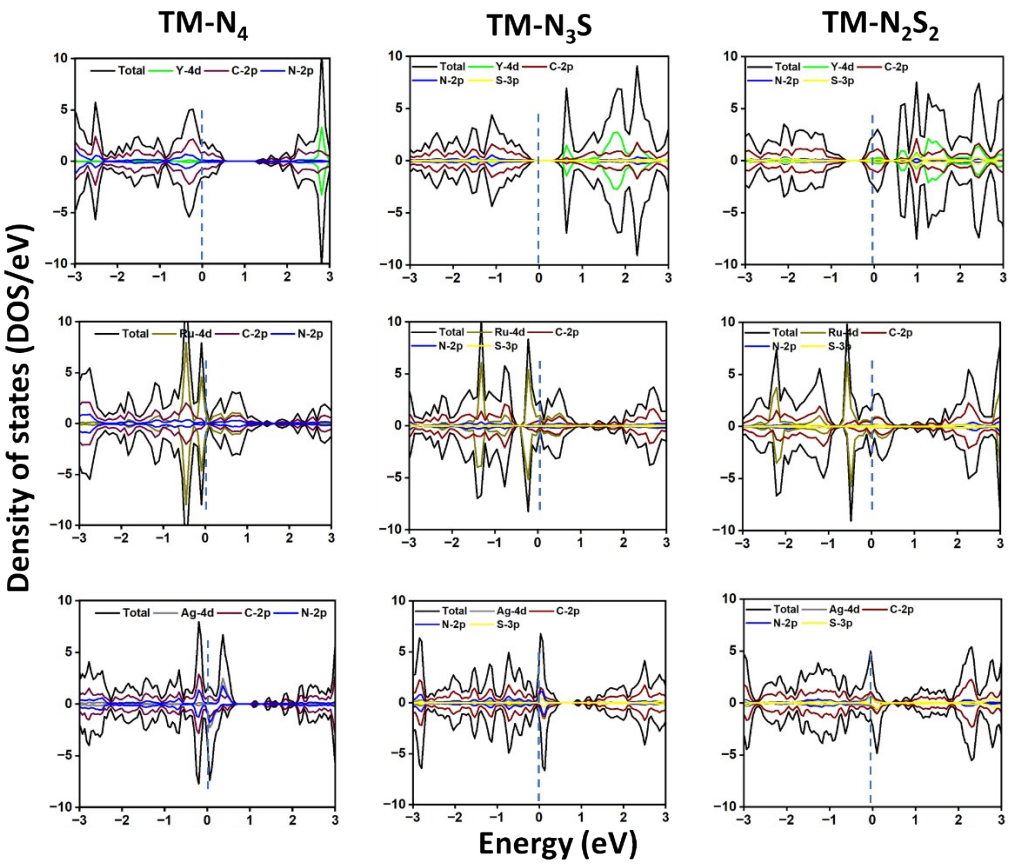

Figure S14. Projected density of states (PDOS) of representative early (Y), mid (Ru) and late (Ag) 4d-TM doped N_4, N_3S and N_2S_2 substrates

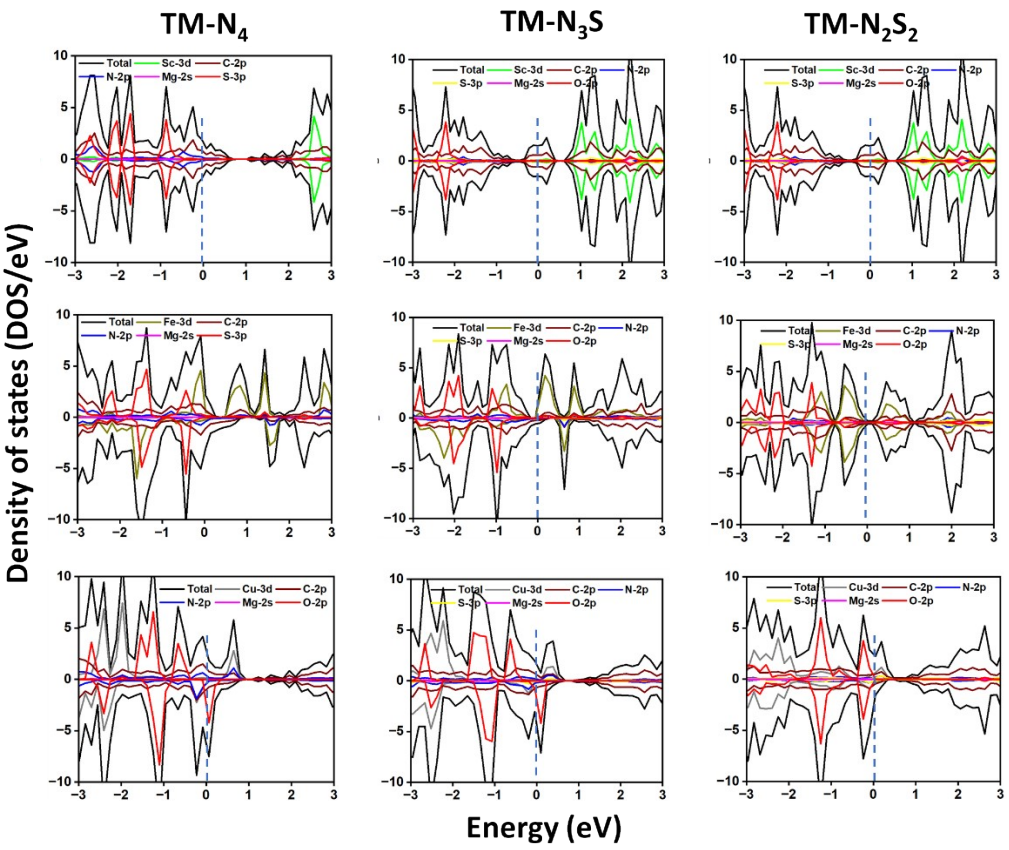

Figure S15. Projected density of states (PDOS) of $MgCO_3$ adsorbed Sc, Fe and Cu TM doped N_4, N_3S and N_2S_2 substrates.

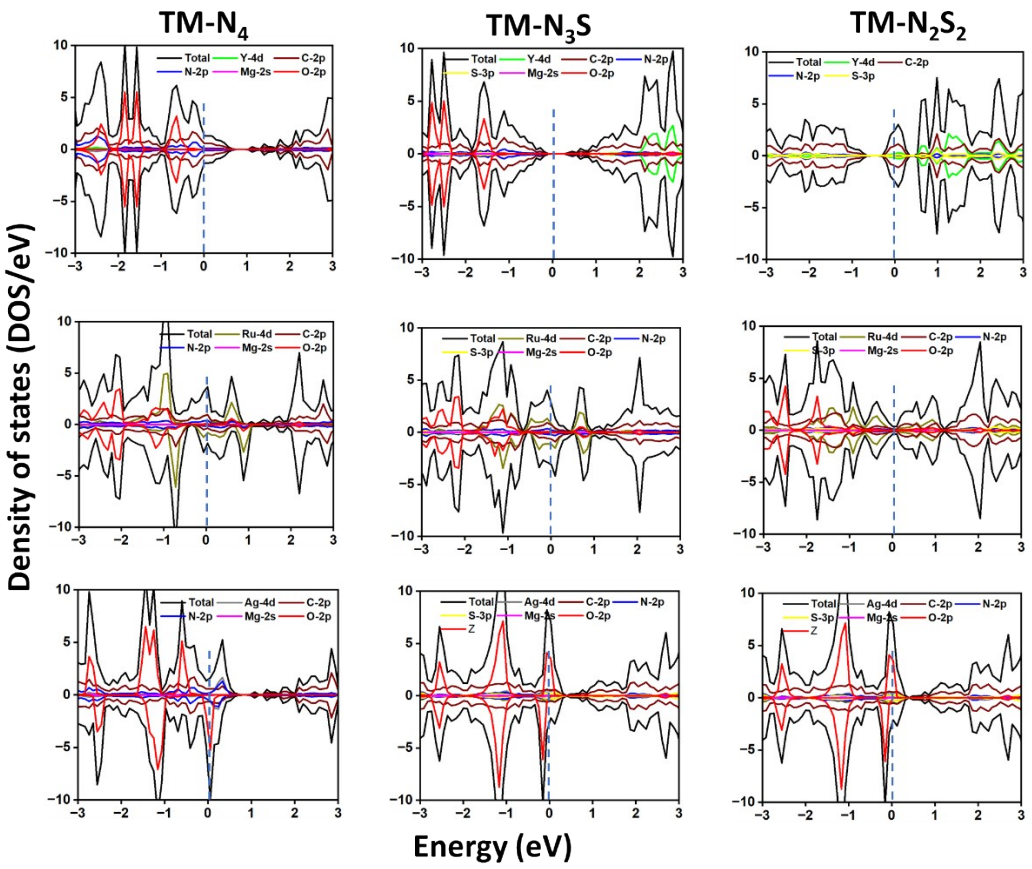

Figure S16. Projected density of states (PDOS) of $MgCO_3$ adsorbed Y, Ru and Ag TM doped N_4, N_3S and N_2S_2 substrates.

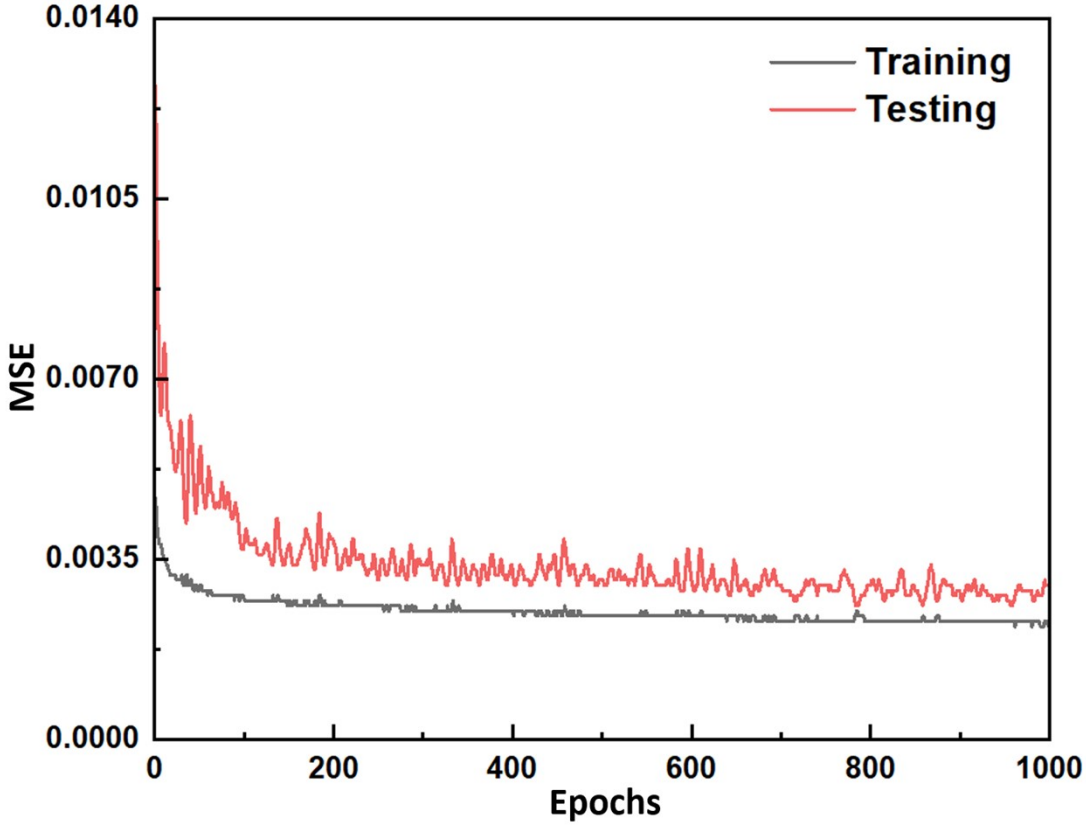

Figure S17. The evaluation of mean square error along with the number of iterations in ANN model

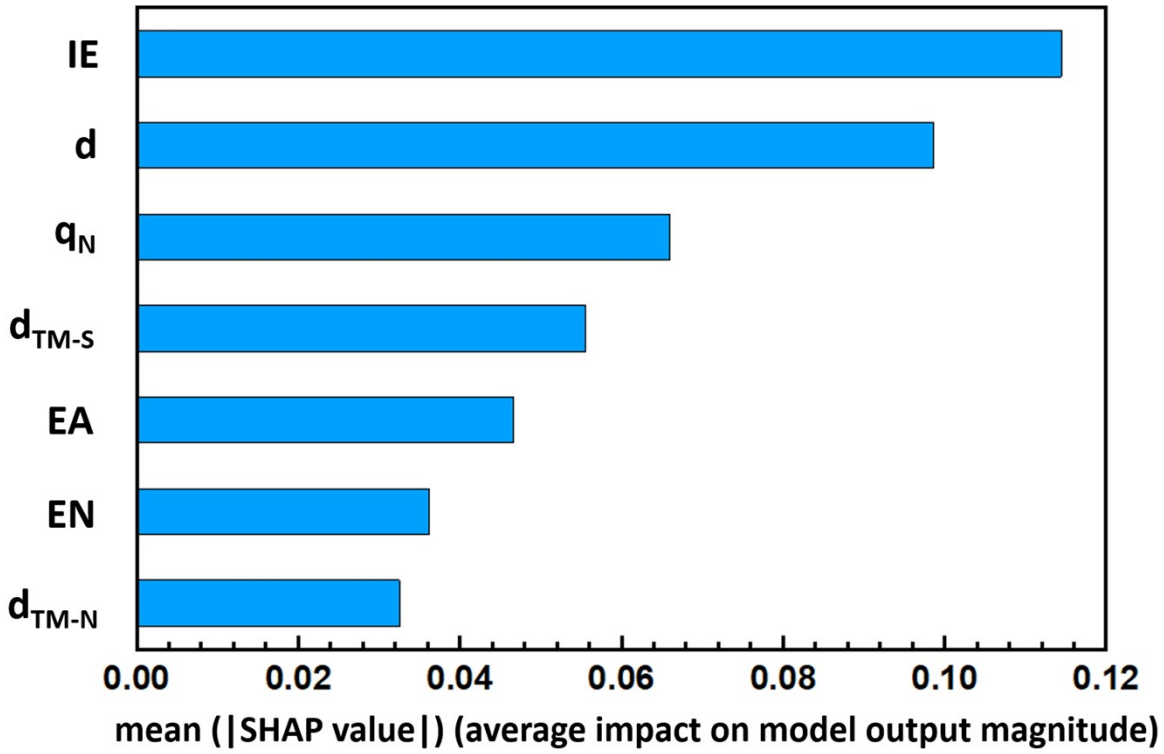

Figure S18. Comparison of SHAP values to analyze the feature importance of ANN model